Under Ricci flow, a 3-torus goes flat

Fixed fibrations, Ricci–DeTurck decay, and three-dimensional collapse

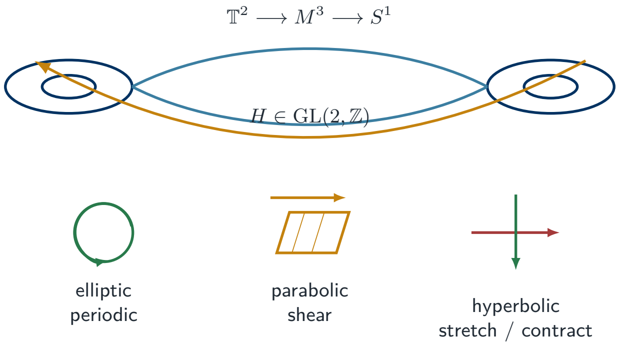

John Lott
University of California, Berkeley

Ricci flow, singularities, and immortal tails

Equation and definition

Ricci flow is

$$\partial_t g = -2\mathrm{Ric}(g).$$

A smooth solution $g(t)$ on a fixed closed manifold M, defined for every $t \in [0, \infty)$, is called *immortal*.

Canonical flow through singularities in dimension three

Starting from any compact Riemannian three-manifold, Kleiner–JL and Bamler–Kleiner give a canonical Ricci flow through singularities. It may become extinct. If it is nonempty for all large times, then after some finite time it is an ordinary smooth Ricci flow on a fixed compact manifold.

So for the long-time behavior, we may consider immortal flows.

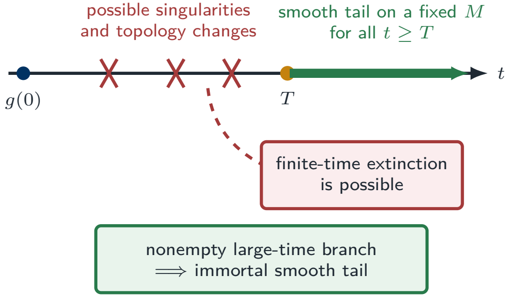

Main theorem

Let M be a closed connected three-manifold admitting a locally homogeneous metric of type $\mathbb{R}^3$, Nil, or Sol, and let $g(t)$ be *any* immortal Ricci flow on M.

$\mathbb{R}^3$ type

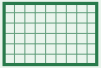

$$g(t) \longrightarrow g_\infty$$

smoothly and exponentially fast, with g_∞ flat.

Nil type

The compact blowdown tends to a point; on $\widetilde{M}$ the limit is

$$\frac{1}{3\tau^{1/3}}\left(dx + \frac{1}{2}y\,dz - \frac{1}{2}z\,dy\right)^2 + \tau^{1/3}(dy^2 + dz^2).$$

Sol type

The compact blowdown tends to a circle or interval; on $\widetilde{M}$ the limit is

$$e^{-2z}\,dx^2 + e^{2z}\,dy^2 + 4\tau\,dz^2.$$

No symmetry is assumed for the initial metric.

The corresponding result for $\mathbb{T}^2$ is due to Hamilton (1988).

Parabolic scaling and Type III behavior

Ricci flow and Type III

Ricci flow satisfies $\partial_t g = -2\mathrm{Ric}(g)$. An immortal flow is *Type III* if

$$\sup_{t\geq 1} t\,\|\mathrm{Rm}(g(t))\|_{L^\infty(M)} < \infty.$$

Thus the curvature scale is at least a constant multiple of $\sqrt{t}$.

Parabolic blowdown

For $s \to \infty$, put

$$g_s(\tau) = s^{-1} g(s\tau).$$

For each s, $g_s(\tau)$ is also a Ricci flow solution. Distances are divided by $\sqrt{s}$, while curvatures are multiplied by s. Hence a Type-III estimate becomes a uniform curvature bound on each fixed τ-interval away from 0.

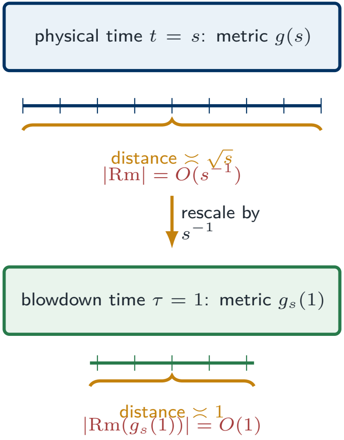

Topology predicts a geometric decomposition

The topological decomposition

1. take the Kneser–Milnor prime decomposition;
2. cut prime factors along incompressible tori, if any (the JSJ tori);
3. each remaining piece carries a locally homogeneous metric modeled on one of Thurston's geometries.

Graph manifolds

A graph manifold is assembled from circle bundles over surfaces. Equivalently, in the prime closed orientable case, it has no hyperbolic pieces.

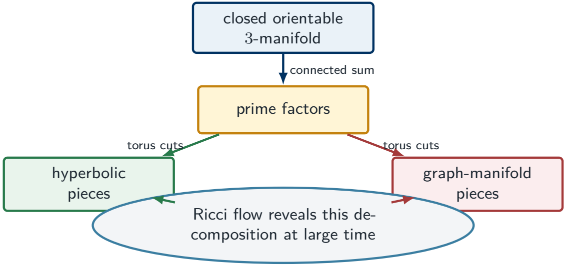

The eight model geometries

S^3 round / spherical	$S^2 \times \mathbb{R}$ sphere along a line	$\mathbb{R}^3$ flat	Nil shearing
Sol stretch / contract	H^3 hyperbolic	$H^2 \times \mathbb{R}$ surface along a line	$\widetilde{\mathrm{SL}}_2(\mathbb{R})$ line over H^2

The long-time viewpoint

Topology supplies the list of possible pieces; Ricci flow is expected to reveal their canonical geometries dynamically.

For compact geometric pieces; finite-volume noncompact hyperbolic and $H^2 \times \mathbb{R}$ pieces can also occur in the full decomposition.

The large-time picture

Canonical Ricci flow

One can flow through singularities. At large time, the connected components are aspherical.

Thick–thin intuition

The thick part looks hyperbolic. The thin part is graph-manifold-like and carries collapsing directions.

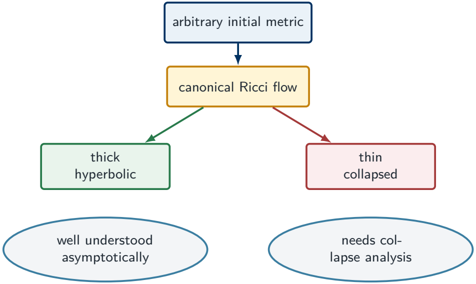

Expected Gromov–Hausdorff limits under $g(t)/t$

Large-time dictionary

Limit of $(M, g(t)/t)$	Thurston type
point	$\mathbb{R}^3$ or Nil
circle/interval	Sol
2-orbifold, $K = -1/2$	$H^2 \times \mathbb{R}$ or $\widetilde{\mathrm{SL}}_2(\mathbb{R})$
3-manifold, $K = -1/4$	H^3

This paper's range

We focus on the torus-bundle geometries: elliptic, parabolic, and hyperbolic monodromy.

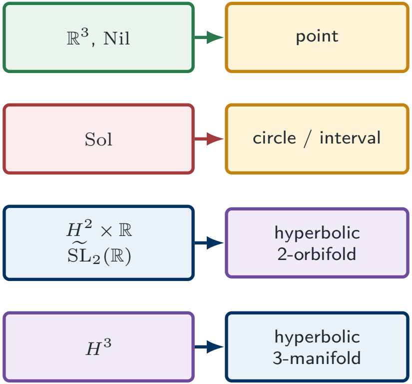

Collapse hides geometry: lift to the universal cover

Compact picture

A collapsing compact limit can be very small: a point, a circle, or an interval.

Lifted picture

The universal cover still remembers the full three-dimensional geometry. Blowdowns of the lifted flow are expected to be expanding solitons.

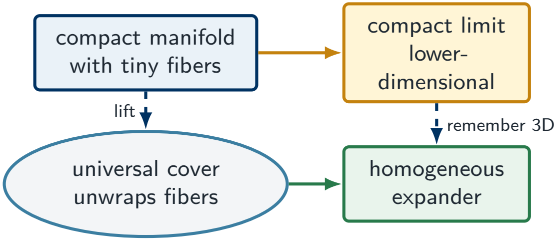

Input I: JL 2010 – identify the blowdown

Hypotheses supplied to the theorem

$$|\mathrm{Rm}_{g(t)}| \leq \frac{C}{t}, \qquad \mathrm{diam}(M, g(t)) \leq C\sqrt{t}.$$

Conclusion used here

The compact blowdown has the dimension predicted by the geometric type, while the lifted blowdown approaches the corresponding homogeneous expanding soliton.

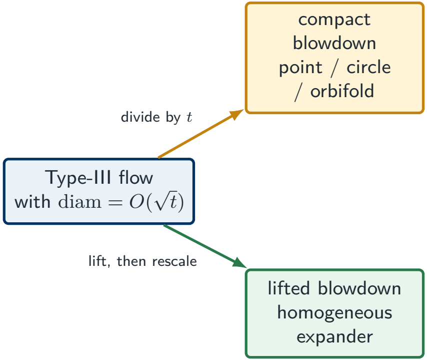

The present paper's job is to prove the diameter bound.

Input II: JL–Sesum – the locally $\mathbb{T}^2$-invariant case

Write a locally $\mathbb{T}^2$-invariant metric over the base coordinate y as

$$g = h_{yy}(y,t)\,dy^2 + G_{AB}(y,t)\,\theta^A\theta^B,$$

where G is the fiber metric and $h_{yy}\,dy^2$ is the quotient metric.

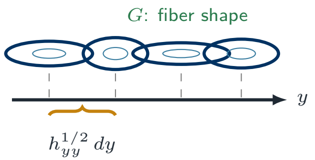

Energy density, energy, and quotient length

$$\mathcal{E}(y,t) = h^{yy}\,\mathrm{Tr}\Big((G^{-1}G_y)^2\Big)\,,$$

$$E(t) = \max_{y\in S^1} \mathcal{E}(y,t),$$

$$L(t) = \int_{S^1} \sqrt{h_{yy}(y,t)}\,dy.$$

Thus $E(t)$ measures the largest normalized variation of the fiber shape along the base, while $L(t)$ is the quotient-circle length.

JL–Sesum estimates

$$\frac{1}{E(t_1)} - \frac{1}{E(t_0)} \geq \frac{1}{2}(t_1 - t_0), \qquad \frac{d}{dt}\log L(t) \leq \frac{1}{4}E(t).$$

The fiber-shape energy decays, and the quotient length can grow only by the accumulated energy.

Input III: Bamler – large-time time-slice structure

For every sufficiently large time

The curvature satisfies

$$\|\mathrm{Rm}(g(t))\|_{L^\infty(M)} \leq \frac{C}{t}.$$

Moreover, there are $\varepsilon(t) \to 0$ and $\lambda_0 > 0$ such that, in the $\mathbb{R}^3$, Nil, and Sol cases, the normalized slice $(M, t^{-1}g(t))$ is $\varepsilon(t)$–GH close to one of

$$\mathrm{pt} \quad \text{(almost flat)}, \qquad S^1_\ell, \qquad [0,\ell],$$

where $\ell \geq \lambda_0$ in the last two alternatives.

The circle branch

The normalized metric is $\varepsilon(t)$-close in high regularity to a locally $\mathbb{T}^2$-invariant model whose torus fibers are very small.

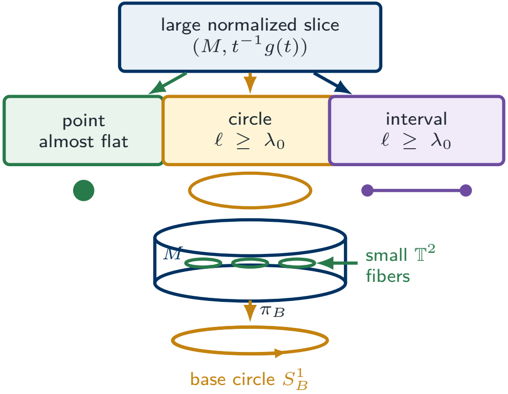

After a finite cover: three possible monodromies

$$M_H = (\mathbb{T}^2 \times [0,1])\big/\big((x,1) \sim (Hx,0)\big), \qquad H \in \mathrm{SL}(2,\mathbb{Z}).$$

case	representative behavior of H	geometry
elliptic	finite order; virtually $H = I$	$\mathbb{R}^3$
parabolic	$\left(\begin{smallmatrix} 1 & m \\ 0 & 1 \end{smallmatrix}\right)$, $m \neq 0$	Nil
hyperbolic	$\lvert \operatorname{tr} H \rvert > 2$	Sol

$$\begin{tikzcd} \boxed{\mathbb{T}^2 \times \{0\}} \arrow[rr, "\text{transport once around } S^1"] & & \boxed{\mathbb{T}^2 \times \{1\}} \arrow[ll, bend left, "H \text{ identifies the ends}"] \end{tikzcd}$$

A torus bundle over a circle

Cut the base circle at one point

The bundle becomes $\mathbb{T}^2 \times [0,1]$. The two boundary fibers are glued by

$$(x,1) \sim (Hx,0).$$

The return map

A loop around the base carries one torus fiber back to itself by $H \in \mathrm{GL}(2,\mathbb{Z})$.

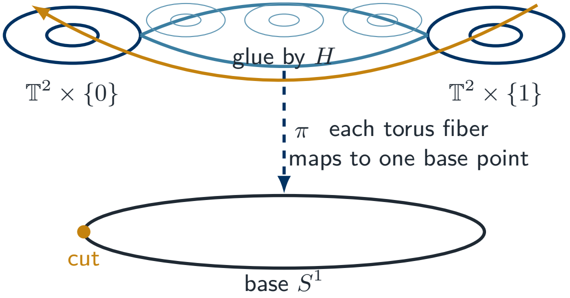

Why time-slice symmetry is not enough

What one large time slice gives

For each large t, Bamler supplies a locally $\mathbb{T}^2$-invariant metric g_t^B that is $\varepsilon(t)$-close to $t^{-1}g(t)$ and has very small torus fibers.

Exact symmetry is understood

When the Ricci flow itself is locally $\mathbb{T}^2$-invariant, the main theorem was proved by JL–Sesum.

The missing spacetime statement

The comparison metric and its preferred fibration may change with t. Without a fixed fiber subgroup and a quantitative contraction between consecutive resets, small errors can accumulate over infinitely many scales.

Time-slice approximation must be upgraded to a coherent stagewise comparison.

Ricci–DeTurck: a heat equation after choosing coordinates

Gauge-fixed equation

Relative to an invariant background Ricci flow $h(t)$, let $q(t)$ solve

$$\partial_t q = -2\mathrm{Ric}(q) + \mathcal{L}_{W(q,h)} q,$$

$$W(q,h)^k = q^{ij}\left(\Gamma(q)^k_{ij} - \Gamma(h)^k_{ij}\right).$$

The principal term is $q^{ij}\nabla_i\nabla_j q$, so the equation is strictly parabolic.

Geometric meaning

Pulling $q(t)$ back by the DeTurck diffeomorphisms recovers the original Ricci flow: the gauge changes coordinates, not geometry.

choose an invariant background $h(t)$

$\downarrow$

obtain a strictly parabolic RDT equation

$\downarrow$

smooth the fiberwise wobble

Averaging over the torus

Given a fixed local $\mathbb{T}^2$-action, split the metric into

$$\text{average} + \text{fluctuation}.$$

The fluctuation is the part that is not invariant along the fibers.

One-stage goal

On a normalized interval $\tau \in [1, 100]$, make the fluctuation at the end much smaller than at the start.

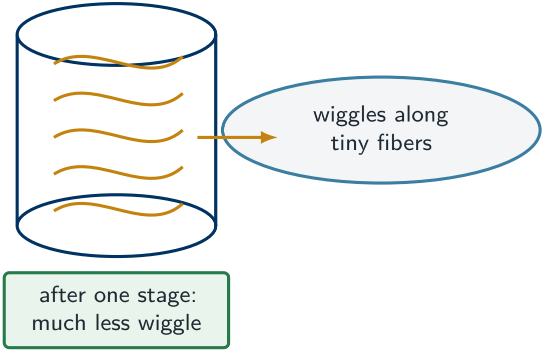

Finite-stage decay of the non-invariant part

Let $h(t)$ be a locally $\mathbb{T}^2$-invariant Ricci flow on $[1, 100]$ with bounded curvature, a nonshort quotient circle, and very short torus orbits. Suppose g_{RDT} remains close to h. For the fixed local torus action, set

$$g_{\mathrm{RDT}}^{\perp} = g_{\mathrm{RDT}} - \mathrm{Av}_{\mathbb{T}^2}(g_{\mathrm{RDT}}).$$

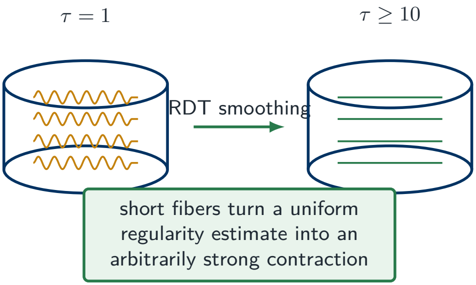

Uniform contraction

For every $\alpha > 0$, if the fibers and initial perturbation are sufficiently small, then

$$\|g_{\mathrm{RDT}}^{\perp}\|_{C^{N+\sigma}(M\times[10,100])} \leq \alpha \, \|g_{\mathrm{RDT}}^{\perp}(1)\|_{C^{N,\sigma}(M)}.$$

The constants remain uniform as the fibers collapse.

Why should the non-invariant part decay?

After parabolic normalization, set $v = g_{\mathrm{RDT}} - h$ and $\rho = \log(t/T_0)$, with h locally $\mathbb{T}^2$-invariant. To first order,

$$\partial_\rho v = \Delta_{L,h} v + \text{bounded lower-order terms.}$$

The leading operator is Lichnerowicz heat flow; high-frequency eigenvalues are taken to be negative.

1. Fourier split on the fiber

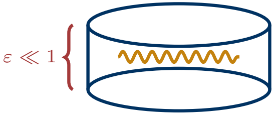

nonzero fiber mode

$$v = \sum_{k \in \mathbb{Z}^2} v_k(y,\rho) e^{ik\cdot\theta}.$$

$k = 0$: invariant; $k \neq 0$: non-invariant.

2. Collapse opens a spectral gap

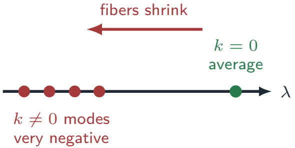

$$\lambda_k \lesssim -c\,|k|^2 \varepsilon^{-2}, \qquad k \neq 0.$$

The non-invariant part lies far to the left.

3. Fast decay in log time

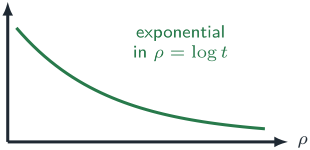

$$\|v^\perp(\rho)\| \lesssim e^{-\gamma(\rho-\rho_0)} = \left(\frac{t}{t_0}\right)^{-\gamma}.$$

Exponential in $\log t$ becomes power decay in t.

Why the contraction is uniform during collapse

On the cyclic cover that unwraps the base, set

$$u = \widehat{g_{\mathrm{RDT}}}, \qquad z_a = u - R_a^* u, \qquad a_0 = \|g^{\perp}_{\mathrm{RDT}}(1)\|_{C^{N,\sigma}},$$
$$w = a_0^{-1} g^{\perp}_{\mathrm{RDT}}, \qquad d = \sup_{\tau \in [1,100]} \mathrm{diam}_h(\text{a local } \mathbb{T}^2\text{-orbit at time } \tau).$$

Translate differences satisfy a local linear equation

For each $a \in \mathbb{T}^2$, mean-value linearization gives

$$\partial_\tau z_a - P_a^{pq} \nabla_p \nabla_q z_a = B_a^p \nabla_p z_a + C_a z_a.$$

Lifted harmonic charts have a fixed radius. Uniform parabolicity, the maximum principle, and Schauder estimates therefore give a high-regularity bound for z_a that is independent of the collapsing scale.

Short orbits turn regularity into smallness

Averaging the z_a recovers w, which has zero orbit average. This gives

$$\|w\|_{C^0} \le Cd\,\|w\|_{C^1}.$$

Interpolation with the uniform high-norm bound gives that for $\tau \in [10, 100]$, for some $0 < \mu < 1$,

$$\|w\|_{C^{N+\sigma}(M \times [10,100])} \le Cd^{\mu}.$$

Hence sufficiently short fibers force an arbitrarily strong contraction.

unwrap the base → compare translates → linearize → Schauder control → short-orbit gain

Fixed-fiber bootstrap: fibers stay small

Geometric claim

If the metric is GH-close to a circle, and the circle base is not too short, then an approximating locally $\mathbb{T}^2$-invariant metric has small fibers.

Why this is useful

The lower bound for the circle base converts Gromov–Hausdorff collapse into the quantitative short-orbit hypothesis needed for finite-stage contraction.

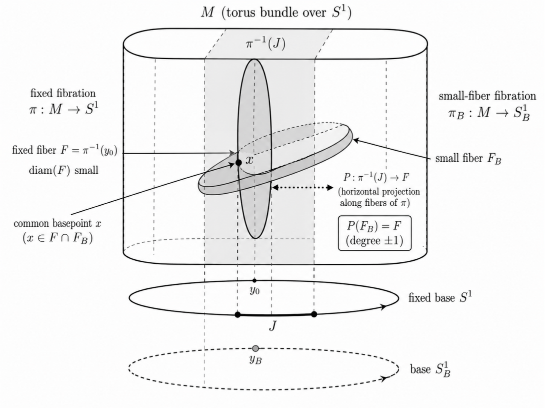

1. start with a controlled metric $q(1)$ at $\tau = 1$;
2. take the average to get $r(1)$;
3. run the Ricci flow to get $r(\tau)$;
4. run the RDT flow starting from $q(1)$, relative to r, to get $q(\tau)$;
5. rescale and restart.

The stage closes

Finite-stage contraction keeps $q(100)$ close to $r(100)$, so the rescaled metric starts the next stage inside the same stability range.

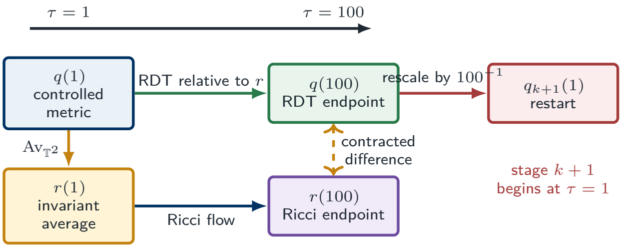

Three flows in the iteration

Fix $T_k = 100^k T_0$ and use normalized time $\tau = t/T_k$ on the kth stage.

Original Ricci flow
$g(t)$ is smooth and geometrically canonical on the immortal tail; no symmetry is assumed.

Continuous piecewise-smooth RDT flow
$g'(T_k\tau) = T_k q_k(\tau)$. Each stage is an RDT pullback of g, and the stages match continuously.

Possibly discontinuous invariant flow
$h(T_k\tau) = T_k r_k(\tau)$. Each r_k is locally $\mathbb{T}^2$-invariant for a fixed fibration structure, but averaging can make h jump at T_k.

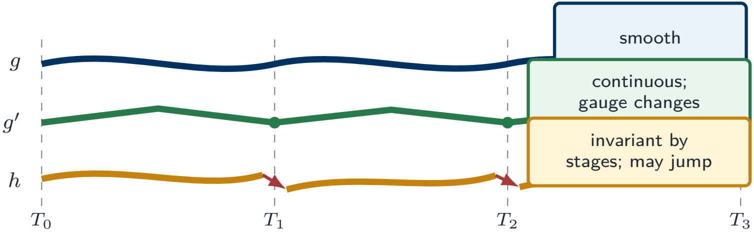

g' is geometrically equivalent to g; the iteration contracts the stagewise error $\|g' - h\|$.

Iteration picture: less wobble at every scale

Spacetime coherence

The induction turns separate time-slice fibrations into one controlled chain of normalized stages.

What to remember

At each restart the metric is closer to its invariant model than it was one stage earlier.

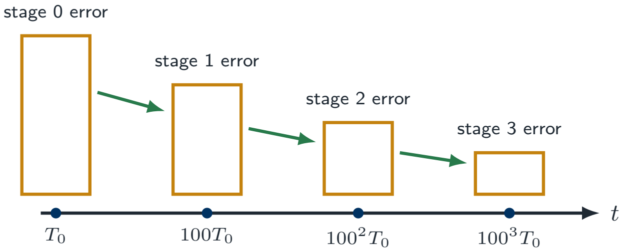

Inside one invariant stage: energy and quotient length

For the invariant stage metric, write

$$r_k = (r_k)_{yy}\, dy^2 + G_{k,AB}\, \theta^A \theta^B .$$

Here G_k is the fiber metric and $(r_k)_{yy} dy^2$ is the quotient metric on the base circle.

Set

$$e_k(\tau) = \max_{S^1} (r_k)^{yy} \operatorname{Tr}\Big(((G_k)^{-1}(G_k)_y)^2\Big), \qquad E_k = e_k(1),$$

$$\ell_k(\tau) = L(S^1, (r_k)_{yy}(\tau)), \qquad \ell_k = \ell_k(1).$$

The JL–Sesum estimates become

$$e_k(\tau) \le \frac{E_k}{1 + \frac{1}{2}(\tau - 1)E_k},$$

$$\ell_k(\tau) \le \ell_k \left(1 + \frac{1}{2}(\tau - 1)E_k\right)^{1/2}.$$

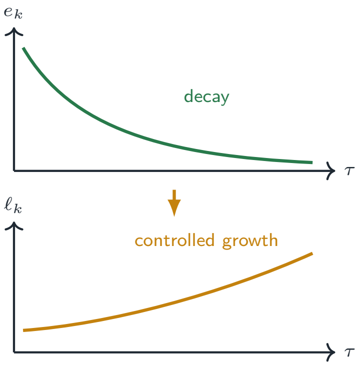

Geometric exchange

The fiber-shape energy decays, while the quotient length grows only by the corresponding controlled factor.

The transition jump and the scalar recursion

After flowing to $\tau = 100$, average the endpoint and rescale by 100^{-1}. If b_k is the non-invariant error, then

$$E_{k+1} \le \frac{100E_k}{1+\frac{99}{2}E_k} + Cb_k, \qquad \ell_{k+1} \le (1+Cb_k)\left(\frac{1+\frac{99}{2}E_k}{100}\right)^{1/2}\ell_k.$$

Energy reset

For

$$F(E) = \frac{100E}{1+\frac{99}{2}E},$$

one has $0 \le F(E) < 200/99$. One stage sends arbitrary energy to a universal range.

Why length remains bounded

The excess above the fixed point $E = 2$ and the jumps b_k are summable. Hence the logarithmic length increments are summable.

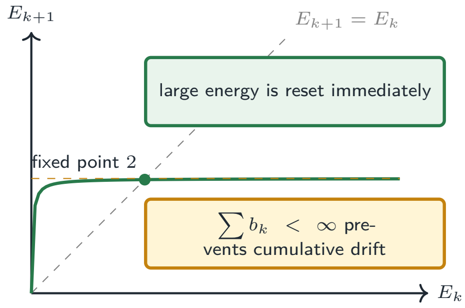

From normalized quotient length to physical diameter

On stage k, the physical comparison metric is

$$h(T_k\tau) = T_k r_k(\tau).$$

Hence

$$L(S^1, h_{yy}(T_k\tau)) = \sqrt{T_k}\,\ell_k(\tau) \le C\sqrt{T_k\tau} = C\sqrt{t}.$$

The fixed fibers are also $O(\sqrt{t})$ in physical scale, and q_k is uniformly bilipschitz to r_k. Therefore

$$\mathrm{diam}(M, g(t)) \le C\sqrt{t}.$$

Elliptic monodromy: flat geometry wins

After a finite cover

The bundle is a 3-torus.

Two possible large-time branches

1. The normalized flow enters an almost-flat region; or
2. the fibred regime persists, and the stagewise argument gives $\mathrm{diam}(M, g(t)) \leq C\sqrt{t}$.

In either case, the $\mathbb{R}^3$ case of JL 2010 yields an almost-flat blowdown; expanding to diameter one and taking a finite cover, along with local stability of flat metrics, then gives smooth convergence to a flat metric.

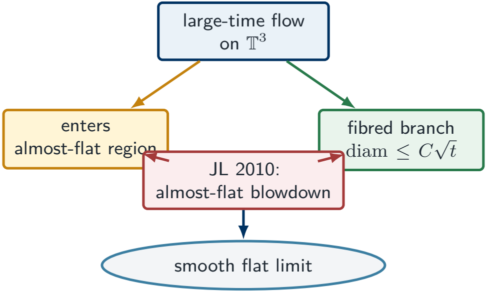

Hyperbolic monodromy: Sol geometry

Topological obstruction to almost flatness

A closed almost-flat manifold is infranil, hence has virtually nilpotent fundamental group. A Sol torus bundle has hyperbolic monodromy and exponential-growth fundamental group. Therefore the flow cannot enter an almost-flat region.

Flow conclusion

The fibred diameter argument applies. JL 2010 then identifies the compact blowdown on the finite cover as a circle, while the lifted flow converges to the Sol expander.

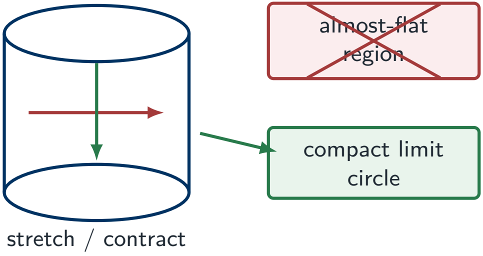

Parabolic monodromy: organize the global Nil dichotomy

In the nontrivial fibred branch, define the normalized diameter

$$\mathcal{D}(t) = t^{-1/2}\mathrm{diam}(M, g(t))$$

and, for fixed $D_0 > 0$,

$$\mathcal{L} = \{t \geq T_{\mathrm{Nil}} : \mathcal{D}(t) \geq D_0\}.$$

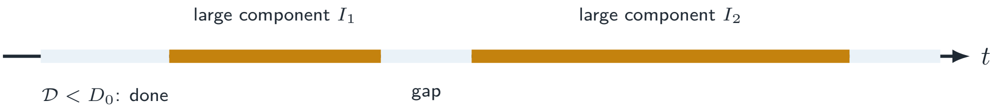

Strategy

The complement $\mathcal{L}^c$ already satisfies the desired diameter bound. On every connected component $I \subset \mathcal{L}$, Bamler's fibred comparison is available at every time, so the fixed-fibration machinery can be run componentwise.

Nil large components: the first block resets the energy

Start a large-normalized-diameter component at time S with

$$\operatorname{diam}(M, g(S)) \leq D_1\sqrt{S}.$$

Type-III metric distortion controls the first block directly; no uniform initial vertical-energy bound is assumed.

Automatic reset

$$E(100^{-1}r_0(100)) \leq \frac{100E_0}{1+\frac{99}{2}E_0} < \frac{200}{99} < 3.$$

After the endpoint jump, E_1 is universally bounded, so the same recursion controls every later complete block.

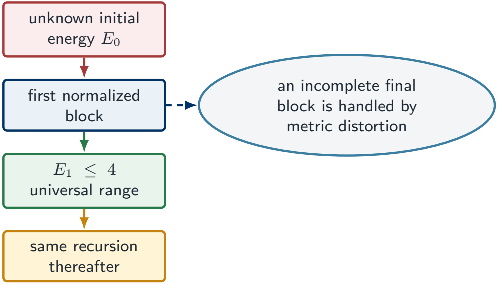

JL's Nil case then gives compact collapse to a point and the Nil expander on $\widetilde{M}$.

What the paper adds

Type-III Ricci flow → time-slice small fibers → fixed-fibration spacetime coherence → $\operatorname{diam} \leq C\sqrt{t}$ → homogeneous blowdown

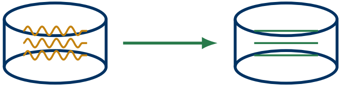

The bridge

Finite-stage Ricci–DeTurck contraction plus the energy–length recursion turns Bamler's time-slice structure into the diameter hypothesis needed by JL 2010.

A remaining conjecture

Conjecture

For an immortal Ricci flow on a closed three-manifold,

$$\operatorname{diam}(M, g(t)) = O(\sqrt{t}) \quad \Longleftrightarrow \quad M \text{ admits a locally homogeneous metric.}$$

The $\Longrightarrow$ direction

The $\Longrightarrow$ direction follows from JL 2010, Proposition 3.5: under the Type-III bound, the square-root diameter estimate forces a single geometric piece.

two one-cusped finite-volume hyperbolic manifolds, truncated and glued

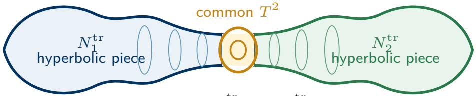

$M = N_1^{\mathrm{tr}} \cup_{T^2} N_2^{\mathrm{tr}}$

H^3	$\mathbb{R}^3$	Nil
✓ known	✓ known	✓ known
Sol	$H^2 \times \mathbb{R}$	$\widetilde{\mathrm{SL}}_2(\mathbb{R})$
✓ known	? open	? open

The $\Longleftarrow$ direction is known for H^3, $\mathbb{R}^3$, Nil, and Sol.

Remaining cases

For $H^2 \times \mathbb{R}$ and $\widetilde{\mathrm{SL}}_2(\mathbb{R})$, the present strategy lacks the needed inputs from both JL–Sesum and Bamler.

Thank you

Questions

Ricci flow → collapse → fixed fibration → blowdown

Proof of Theorem 3: Indefinite Ricci–DeTurck iteration

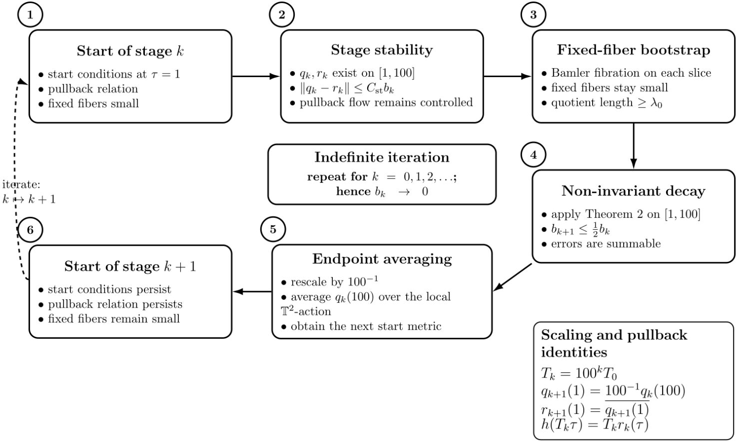

Backup: full energy–length recursion

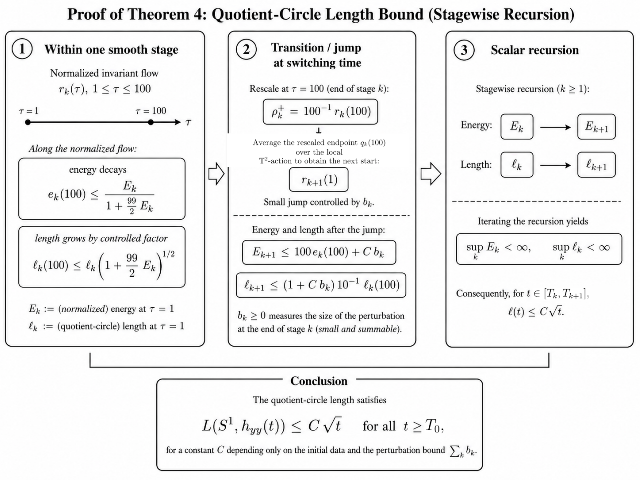

Backup: mean-value linearization

On the cyclic cover, set $u = \widehat{g}_{\mathrm{RDT}}$, $u_a = R_a^* u$, and $z_a = u - u_a$. Along

$$u_s = u_a + s(u - u_a), \qquad 0 \le s \le 1,$$

the fundamental theorem of calculus gives

$$\mathcal{Q}_{\widehat{h}}(u) - \mathcal{Q}_{\widehat{h}}(u_a) = \int_0^1 D\mathcal{Q}_{\widehat{h}}|_{u_s}[z_a]\, ds.$$

Thus

$$\partial_t z_a - P_a^{pq} \nabla_p \nabla_q z_a = B_a^p \nabla_p z_a + C_a z_a,$$

with

$$P_a^{pq} = \int_0^1 u_s^{pq}\, ds, \qquad B_a^p = \int_0^1 \mathcal{B}_s^p\, ds, \qquad C_a = \int_0^1 \mathcal{C}_s\, ds.$$

The principal coefficient is uniformly elliptic because every u_s is uniformly bilipschitz to $\widehat{h}$.

Backup: regularity of the linearized coefficients

For

$$\partial_t y - P^{pq}\nabla_p\nabla_q y = B^p\nabla_p y + Cy,$$

the mean-value coefficients along u_s have the formal parabolic regularities

$$P \in C^{N+\sigma,(N+\sigma)/2}, \quad B \in C^{N-1+\sigma,(N-1+\sigma)/2}, \quad C \in C^{N-2+\sigma,(N-2+\sigma)/2}.$$

Schematically,

$$B \sim u^{-1} * u^{-1} * \nabla u,$$

$$C \sim u^{-2} * \nabla^2 u + u^{-3} * \nabla u * \nabla u + \mathrm{Rm}(h) * \mathcal{A}(u, u^{-1}).$$

On any interior slab $[1+\delta, 100]$, Shi estimates for h and quasilinear Schauder estimates for u give all higher coefficient bounds required by the nested-cylinder bootstrap.

Backup: maximum principle and Schauder estimates

For $y_a = z_a / \|g^{\perp}_{\mathrm{RDT}}(1)\|$ and $\phi_a = |y_a|^2_{\widehat{h}(t)}$,

$$(\partial_t - P_a^{pq}\nabla_p\nabla_q)\phi_a \leq C\phi_a.$$

The deck generator conjugates the torus translations by the monodromy, so $(x, a) \mapsto \phi_a(x, t)$ descends to a compact associated bundle. The scalar maximum principle gives a uniform C^0 bound. On the universal cover, the invariant background $h(t)$ has a fixed-radius harmonic-coordinate atlas. This uses:

- the universal-cover injectivity-radius estimate;
- curvature bounds and Shi derivative estimates;
- control of $\partial_t h = -2\mathrm{Ric}(h)$.

In these charts the system is uniformly parabolic with controlled Hölder coefficients. Nested backward-cylinder Schauder estimates give the required high-order bounds; at $t = 100$ one uses a one-sided backward cylinder.

Backup: why the injectivity-radius lemma is enough

The universal-cover lemma says: if g has bounded curvature and is uniformly bilipschitz to a locally invariant torus-bundle metric h, then

$$\mathrm{inj}_{\tilde{g}} \geq i_B \Lambda^{-1/2}.$$

Its uses are different in the two analytic arguments.

1. In the decay theorem, take $g = h$: the invariant background supplies the harmonic-coordinate atlas. The unknown Ricci–DeTurck metric only needs to be uniformly close to h.
2. In stage stability, the generally non-invariant reference flow $p(\tau)$ is bilipschitz to Bamler's invariant comparison m_τ, so the lemma applies directly to $p(\tau)$.
3. In the second comparison, the reference $r(\tau)$ is itself invariant.

Injectivity radius supplies a spatial radius; curvature bounds, Shi estimates, and control of $\partial_t g = -2\mathrm{Ric}$ supply the full parabolic Schauder atlas.

Backup: the stage-stability estimate

Let $p(\tau)$ be the normalized original Ricci flow on $[1/2, 101]$ and let

$$r(1) = \overline{p(1)}.$$

For sufficiently small

$$b = \|p(1) - r(1)\|_{C^{N,\sigma}(M,r(1))},$$

the invariant Ricci flow $r(\tau)$ exists on $[1, 100]$, and the Ricci–DeTurck representative $q(\tau)$ of $p(\tau)$ relative to $r(\tau)$ satisfies

$$\|q - r\|_{C^{N+\sigma,(N+\sigma)/2}} \leq C_{\mathrm{st}} b.$$

The proof uses a common continuous-dependence estimate

$$\|u\|_{X_s(T)} \leq C_0\big(\|u(1)\|_{C^{N,\sigma}} + \|\mathcal{L}_s u\|_{Y_s(T)}\big),$$

with a quadratic Taylor remainder

$$\|\mathcal{N}_s(u)\|_{Y_s(T)} \leq C\|u\|^2_{X_s(T)},$$

followed by a bootstrap and continuation argument.

Backup: transition estimates under a collapsing fiber scale

For two nearby invariant metrics ρ and $\widetilde{\rho}$, use a horizontal gauge for ρ and normalized horizontal/vertical frames. Relative $C^{N,\sigma}$ control bounds

$$\frac{\widetilde{a}}{a}, \qquad G^{-1/2}(\widetilde{G}-G)G^{-1/2},$$

$$a^{-1/2}G^{-1/2}\partial_y(\widetilde{G}-G)G^{-1/2}$$

independently of the absolute fiber scale. Consequently, if $E(\rho) \le E_0$ and $\delta = \|\widetilde{\rho}-\rho\|_{C^{N,\sigma}(\rho)}$ is small,

$$E(\widetilde{\rho}) \le E(\rho) + C\delta, \qquad L(\widetilde{\rho}) \le (1+C\delta)L(\rho).$$

This scale-free estimate is what allows endpoint averaging during collapse.

Backup: exact closure of the scalar recursion

The fixed point $E = 2$ is visible from

$$F(E) - 2 = \frac{E - 2}{1 + \frac{99}{2}E}.$$

With $y_k = (E_k - 2)_+$,

$$y_{k+1} \le \frac{1}{100} y_k + C b_k, \qquad \Longrightarrow \qquad \sum_k y_k < \infty.$$

Moreover,

$$\left(\frac{1 + \frac{99}{2}E_k}{100} \right)^{1/2} = \left(1 + \frac{99}{200}(E_k - 2) \right)^{1/2},$$

so

$$\log \frac{\ell_{k+1}}{\ell_k} \le C(y_k + b_k).$$

Since both series on the right are summable,

$$\sup_k E_k < \infty, \qquad \sup_k \ell_k < \infty.$$

Selected references

- B. Kleiner and JL, *Singular Ricci flows I*, Acta Math. 219 (2017), 65–134.
- R. Bamler and B. Kleiner, *Uniqueness and stability of Ricci flow through singularities*, Acta Math. 228 (2022), 1–215.
- G. Perelman, *The entropy formula for the Ricci flow and its geometric applications* (2002); *Ricci flow with surgery on three-manifolds* (2003).
- JL, *Dimensional reduction and the long-time behavior of Ricci flow*, Comment. Math. Helv. 85 (2010), 485–534.
- JL and N. Sesum, *Ricci flow on three-dimensional manifolds with symmetry*, Comment. Math. Helv. 89 (2014), 1–32.
- R. Bamler, *Long-time behavior of 3-dimensional Ricci flow. Introduction*, Geom. Topol. 22 (2018), 757–774.

Additional analytic references

- D. DeTurck,
  Deforming metrics in the direction of their Ricci tensors,
  J. Differential Geom. 18 (1983), 157–162.
- W.-X. Shi,
  Deforming the metric on complete Riemannian manifolds,
  J. Differential Geom. 30 (1989), 223–301.
- O. Ladyzhenskaya, V. Solonnikov, and N. Ural'tseva,
  Linear and quasilinear equations of parabolic type,
  AMS Translations of Mathematical Monographs 23 (1968).
- M. Gromov,
  Almost flat manifolds,
  J. Differential Geom. 13 (1978), 231–241.
- J. Cheeger, M. Gromov, and M. Taylor,
  Finite propagation speed, kernel estimates, and the geometry of complete Riemannian manifolds,
  J. Differential Geom. 17 (1982), 15–53.